Proceedings of the 17th World Congress
The International Federation of Automatic Control
Seoul, Korea, July 6-11, 2008

Development, Control and Evaluation of a Mobile Platform for Microrobots

Christoph Edeler, Daniel Jasper, Sergej Fatikow

Division Microrobotics and Control Engineering, University of Oldenburg, Germany (phone: +49-441-798-4296; e-mail: christoph.edeler@informatik.uni-oldenburg.de)

Abstract: This paper describes the development, control and evaluation of a mobile platform for microrobots. The platform uses laser-structured piezoceramic plates equipped with ruby hemispheres in order to continuously rotate three steel spheres using the stick-slip effect. The spheres roll on the working surface and can thus move the platform in two translational and one rotational degrees of freedom. This indirect stick-slip actuation does not stress the working surface and can even operate on surfaces that are not perfectly flat. The exact geometry of the actuators is analyzed and an open-loop control approach is derived. As there are 27 piezo segments moving nine ruby hemispheres and three steel spheres, both the amplification hardware and the software algorithms need to be carefully designed. A prototype was built and evaluated to prove the concept. Basic data about the platform's properties such as step length, resolution and actuation speed was gathered. The results are very promising as the platform can move with nm-resolution and with velocities of up to 10 mm/s.

1. INTRODUCTION

For microsystem technology, the manipulation of objects in the micro- and nanoscale is a major challenge. There are different demands on manipulators in the fields of nanotechnology, material research, in the semiconductor industry, and for research topics in biological sciences or medicine. The term "manipulation" in this case ranges from "simple" positioning with predictable exactness to multidimensional, complex nano/microassembly tasks.

Conventional industrial drives, e.g. stepper motors with elevating screws or gearboxes, can hardly meet the requirements of an adequate positioning in the nanometer range. Systems based on these techniques achieve sub-μm accuracies (Burisch et al. [2004]), but are unable to support higher resolutions due to disturbing effects such as friction, backlash, thermal expansion, and effects coming from accelerating high masses, e.g. in direct-current (DC) motors. Even with high efforts, disturbing effects cannot be eliminated without degrading other properties, e.g. an increased cross-section which makes the use in space-limited environments impossible.

The lack of flexibility is another drawback of conventional systems. Nearly every existing system is designed with a high level of specialization and can therefore not be adapted easily to different requirements. This especially applies to manipulators built for nano-manufacturing, because specialization is needed to perform tasks.

For robot-based manipulations in the nanometer range, drives with high accuracy are necessary. Furthermore, manipulations in the nanoscale are mainly carried out within the vacuum environment of a Scanning Electron Microscope (SEM), which is small compared to conventional robotic drives. Thus, drives with high accuracy, high flexibility and adequately small dimensions are needed. The robotic research community as well as industry has done research in this field (Kim et al. [2001], Fatikow et al. [2000], Martel et al. [2000]). Mainly, two solutions are traced:

(1) Development of linear actuators featuring one degree of freedom (DoF) and building positioning devices based on Cartesian coordinates. This solution is followed by both industry, e.g. N.N. [2007], and research (Breguet et al. [1996]).
(2) Development of mobile platforms featuring three DoF, two of which are transitional (x and y) while the other is rotational (θ). This solution is only followed by research (Martel and Hunter [2004], Bergander et al. [2004], Driesen et al. [2005], Aoyama [1998]).

A promising concept is the use of small flexible microrobots. These microrobots have dimensions of a few cm^3 and offer modularity and the possibility for manipulation either under an optical light microscope or in the vacuum chamber of an SEM. In the first case, μm-resolution is enough because it is similar to the microscope's resolution. In the latter case, full positioning capabilities down to single nanometers are utilized. As described in Fatikow [2004], microrobots can be divided into: Mobile platform, manipulator and endeffector. This paper describes a driving principle for mobile platforms.

2. WORKING PRINCIPLE

The working principle of the newly designed mobile platform is derived from the Rollbot platform (Kortschack and Fatikow [2004], Fahlbusch et al. [2003]). This platform uses piezo-actuators to rotate steel spheres using stick-slip actuation. Thus, the stick-slip effect takes place on the surface of the steel sphere and does not affect the working surface. As the mobile platform lies on three independently

controllable steel spheres, the platform can be moved in three DoF. The new platform combines this principle with very rigid, specially designed piezoceramic actuators. Furthermore, the exact geometric conditions of the whole actuation is carefully analyzed. The piezoceramics, which are the basis for the actuators, consist of a plate with dimensions of $10 \cdot 10 \cdot 0.5\,\mathrm{mm}^3$. The material is a "soft" lead zirconate - lead titanate ceramic with convenient properties, and the direction of polarization is vertical to the boards plain (z-axis). The plates are delivered with an electrically conductive coating, which is structured to form electrodes and solder pads for the actuators. Fig. 1 compares drive sections of Rollbot and of the new design.

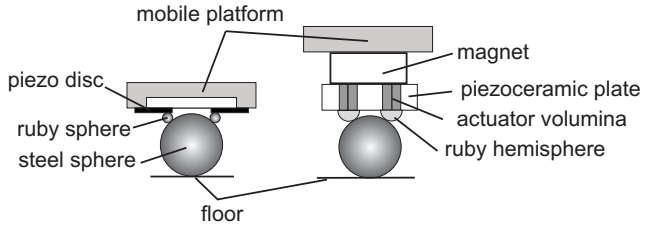

Fig. 1. Schematic of one of three drive sections of the mobile platform, left: Rollbot, right: new design.

Rollbot uses a piezo bending actuator to drive ruby spheres and thereby the steel spheres. A great advantage of this principle is the cheap and easy to build design. Because of the bending actuators, comparatively low voltages of 35 V are enough to get the stick-slip-principle to work. A single step has the size of about 110 nm. However, due to the bending actuators and comparatively large accelerated masses, the system exhibits low resonance frequencies. This makes a control with more than 700 Hz impossible, as described in Hülsen [2007]. Another disadvantage is the impact of a mechanical load which bends the actuators and displaces the platform towards the floor. The new working principle makes use of specially designed piezoceramic actuators. These rotate ruby hemispheres around their center instead of displacing them. Therefore, the steel spheres are actuated while neither ruby hemispheres nor steel spheres change their position. The working principle can be subdivided into three layers: actuator layer, sphere layer, and platform layer.

2.1 Actuator Layer

The actuator layer incorporates the piezoelectric plate and the ruby hemispheres. Fig. 2a) shows the structure of the piezoceramic plate for a single hemisphere, which is fixated to the center of electrodes. The three electrodes can be connected to any potential while the unstructured back of the plate is connected to ground. Thus, the ruby hemisphere is actuated via three channels. Fig. 2b) shows the actuator in a sectional drawing. For simplicity, the working principles in Fig. 2b) and 2c) are drawn "symmetrically", i.e. as if there were only two electrodes for a hemisphere. The ruby hemisphere is attached to the electrodes with an adhesive. The comparably elastic adhesive functions as a joint between the rigid elements ruby and ceramic. By applying a potential to an electrode, the piezoceramic segments expand or contract in z-direction, depending on the polarization direction and the potential's sign (Fig. 2c).

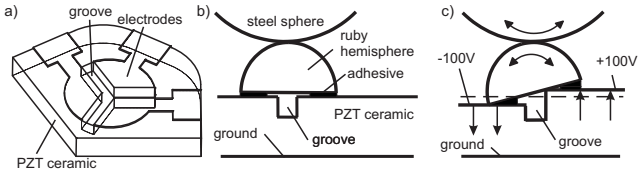

Fig. 2. a) Structured ceramic plate, b) actuator design in static state, c) symmetric potential applied.

Using all three segments, the hemisphere can be elevated and rotated. Elevation is created by applying the same potential to all three segments, but is not required for the working principle. For a rotational movement of the hemisphere, the sum of the displacements must equal zero, e.g. one electrode elongates by 50 nm while the others contract by 25 nm. In reality, the movement will not be purely rotational, because the adhesive does not form geometrically ideal joint points and the piezo segments will not perform a purely vertical movement. In order to focus on the working principle, however, these problems will not be regarded in the following. Instead, it is assumed that ideal rotations of the ruby hemisphere can be generated by applying appropriate potentials.

The fabrication of the piezoceramic structure is done by a Nd-YAG low-power laser. It has a maximum beam power of 8 W, and the focus point is less than 10 μm in diameter. In combination with a three-axis positioning table and a computer numeric control (CNC) software, it is possible to define arbitrary geometric shapes that are then transfered to the piezoceramic. The processing is subdivided into two parts: The forming of electrodes, circuit paths and solder pads in the electrically conductive coating (actuator segmentation). This process step runs with reduced power. It removes the coating, where electrically conductive structures are unnecessary. The second part stands for the structuring of the piezoceramic in depth (actuator structuring). This process step creates the groove in the material (Fig. 2). The groove reduces mechanical stress and constricts geometrical areas of the joints. The process is very flexible and can be adapted, e.g. for further miniaturization. No problems with unintentional short circuits occurred.

The advantage of using a structured piezoceramic plate is the high rigidity. The force flow from the platform to the floor is direct, without any bending or other elastic elements. The accelerated masses are very small. Furthermore, the actuation displacements are smaller. For the Rollbot platform, displacements of several micrometers were used. In this new design a voltage of 100 V leads to an electrode displacement of about 50 nm, according to the piezoelectric charge constant ($d_{33} = 500 \cdot 10^{-12}\,\mathrm{C/N}$). Due to these properties, the critical resonance modes shift to much higher frequencies. Thus, higher stick-slip control frequencies and therefore higher velocities should be possible.

2.2 Sphere Layer

Fig. 1 (right) shows a drive section of the mobile platform. It consists of the piezoceramic actuator with three ruby hemispheres from the actuator layer. A steel sphere lies under the ruby hemispheres, and is held in place by

a permanent magnet. The magnet has a major impact on the slip-stick properties and improves the manual handling, because the steel sphere clings to the platform. The steel sphere is the driven element connecting the mobile platform to the working surface. Now, the ruby hemispheres move in such a manner that a rotation of the steel sphere in two degrees of freedom is achieved (see section 3).

An important consideration are the position and the properties of the stick-slip contact point. It must be ensured that the stick-slip effect occurs between ruby hemisphere and steel sphere and not between steel sphere and working surface. Otherwise the important benefit of the internal stick-slip would be lost. Furthermore, the effect should be sufficiently independent of the load in order to create a versatile platform. Lastly, the stick-slip effect should be usable at high control frequencies to obtain usable speeds.

The conditions of force and friction of the stick-slip contact are critical for the effect. Fig. 3 sketches the different forces used for actuation.

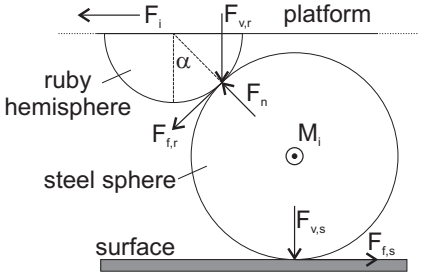

Fig. 3. Normal and friction forces acting during platform operation.

The friction force $F_{f,r}$ between ruby hemisphere and steel sphere depends on the vertical force $F_{v,r}$ of a ruby hemisphere and the angle of the contact point α. The force $F_{v,r}$ depends on the mass m_p of the platform as well as the employed permanent magnet. The friction force $F_{f,s}$ of a single steel sphere is a result of the force $F_{v,s}$ depending on the mass of the platform m_p and the mass of the steel sphere m_s. The friction is modeled as Coulomb friction with the coefficients μ_r and μ_s. This model might not accurately match the real, non-linear friction behavior, but is a sufficient approximation to understand the following considerations.

In order for the stick-slip effect to work, two conditions must be fulfilled. Firstly, for the slip phase, $F_{f,r}$ must be very small, so that the inertia momentum M_i of the steel sphere is not overcome. Thereby, the steel sphere will remain in place while the ruby hemisphere is moved. This also ensures that the steel sphere does not slip on the surface. Secondly, during the stick phase, $F_{f,r}$ must be high enough to overcome M_i as well as the inertia force F_i created by the mass of the platform.

Without a permanent magnet, only relatively slow stick phases and, thus, low control frequencies are possible. If the stick phase is too fast, M_i and F_i will be to large to be overcome by $F_{f,r}$. $F_{f,r}$ could be increased by increasing the mass of the platform and thus creating a higher vertical force $F_{v,r}$, but this would also increase F_i. With friction coefficient μ and acceleration of gravity g the formulas are:

$$F_i = m_p \cdot a \tag{1}$$

$$F_{f,r} = \mu_r \cdot F_n = \mu_r F_{v,r} \cdot \cos\alpha = \mu_r \cdot m_p g \cdot \cos\alpha \tag{2}$$

According to (1) and (2), both F_i and $F_{f,r}$ increase linearly with the platform's mass. Thus, no significant change in their proportion can be achieved and the maximum stick speed cannot be increased. Adding a permanent magnet, however, allows increasing $F_{v,r}$ and $F_{f,r}$ without significantly increasing m_p and F_i. Therefore a higher stick speed is possible and the control frequency can be increased. Taking the linear relation between $F_{f,r}$ and m_p into account, the platform should show a movement behavior that is independent of the platform's mass. However, an increased mass will also increase $F_{v,s}$ and thus the friction of the steel sphere on the surface $F_{f,s}$. If the platform is too light, external forces, e.g. exerted by cables, can stop the movement although the steel sphere still rotate.

2.3 Platform layer

The third layer of actuation is the platform itself. It is driven by three drive sections. The control of three independent steel spheres from the sphere layer leads to a platform motion in three degrees of freedom.

The prototype shown in Fig. 4 consists of a printed circuit board that has milled holes that exactly fit the 0.5 mm thick laser-structured ceramic plates. Thereby, the ceramics are well aligned in an equilateral triangle. The permanent magnets are embedded into the opposite side of the circuit board so that they touch the other side of the ceramic.

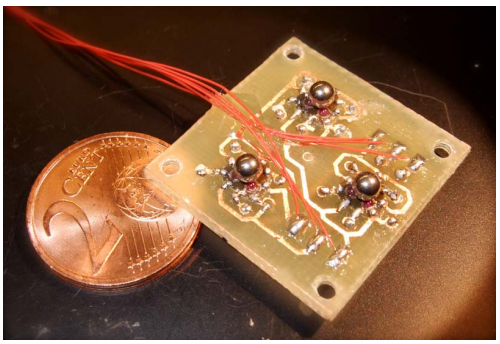

Fig. 4. Prototype of the mobile platform.

The prototype's width and length are 25 mm and the size can easily be reduced to less then 20 mm. The employed chrome steel spheres have a 3 mm diameter, and the overall platform height is 6 mm.

3. CONTROL

There are several problems and design decisions when controlling the mobile platform. Firstly, the three channels of a single ruby hemisphere in the actuator layer have to be controlled in order to obtain two rotational degrees of freedom. Secondly, each of the three ruby hemispheres has to be controlled in two degrees of freedom in order to create

a rotation of a steel sphere. Lastly, three steel spheres have to be controlled in order to obtain the three degrees of freedom in the platform layer.

3.1 Control of a ruby hemisphere

As mentioned in section 2, there are three individual channels that have to be controlled for each ruby hemisphere (Fig. 5a). As a simplification, the contact point between ruby hemisphere and actuator segment is assumed to be a single point in the center of the segment. Thus, the ruby hemisphere is supported by three individually controllable points that form an equilateral triangle (Fig. 5b). Each of these points can be moved vertically by applying a voltage to the corresponding segment. The distance of movement is called d_i, where positive values stand for an elongation of the segment. Not taking non-linear effects of piezo-based actuation such as hysteresis and drift into account, d_i is proportional to the applied voltage. The maximal possible value $|d_{max}|$ is limited by the maximum voltage. In order to create a purely rotational movement of the ruby hemisphere, the sum of the d_i has to equal 0. In that case, the triangle's center of gravity, which is also the center of the hemisphere, does not move.

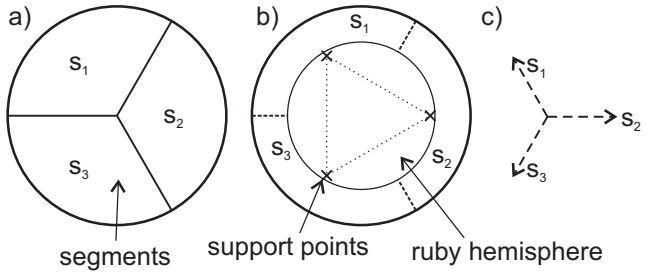

Fig. 5. a) Three segments for a hemisphere, b) hemisphere is supported by three points, c) simplified drawing.

The simplified drawing in Fig. 5c) only shows the direction of movement that is created with the corresponding segment. The ruby hemisphere can theoretically be rotated into an arbitrary direction. As a simplification, however, only two special cases are considered here. In the first case, one segment is connected to ground, one is connected to a posive voltage U, and one is connected to -U (see Fig. 6a). In the other case, one segment is connected to U, while the other two segments are connected two a negative voltage with half the value $-\frac{1}{2}U$ (see Fig. 6b). Taking all symmetries into account, the ruby hemisphere can be moved into 12 directions with a spacing of 30 degrees between them using these two cases.

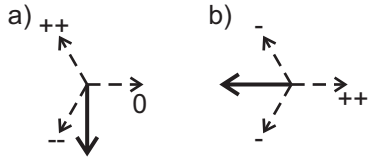

Fig. 6. a) movement using two electrodes, b) movement using three electrodes

For the controller and amplifier, it is an additional challenge to ensure that the sum of the applied potentials equals zero. Even for the special cases shown in Fig. 6, two voltage levels are necessary. However, this problem can easily be avoided by not connecting the other side of the piezo plate to the signal ground. Instead, an unconnected circular electrode is structured for each triplet of segments. This electrode acts as a charge divider (Fig. 7).

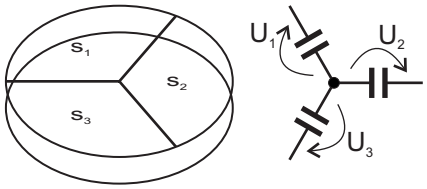

Fig. 7. Actuator segments with unconnected electrode on the other side.

All segments are structured with the same size and have similar wiring. Thus, they all have the same capacitance and the sum of the voltages always equals zero:

$$U_1 + U_2 + U_3 = 0 \tag{3}$$

Fig. 8 shows the voltages, that are created if a movement as in Fig. 6b) is created. There is no need to create different voltage amplitudes for the different signals, as the charge is automatically divided as required. In the unconnected electrode, a potential of $-50\,\mathrm{V}$ is created, and the voltage on the positive segment is twice as high as the voltage on the two negative segments.

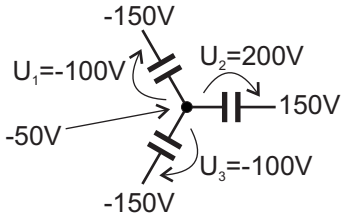

Fig. 8. Example of charge division.

3.2 Control of a steel sphere

In order to control a single steel sphere, the interaction between ruby hemisphere and steel sphere has to be carefully analyzed. The first important consideration is the geometric position of their contact point. The prototype uses ruby hemispheres with 1 mm diameter and steel spheres with 3 mm diameter. The three hemispheres are arranged in a circle with 1.3 mm radius. Therefore, the contact point, the center of the hemisphere and the hemisphere's topmost point form a 40.54-degree angle (see Fig. 3). The same applies to the contact point on the steel sphere and its bottommost point. Thus, a straight line can be drawn from the steel sphere's center through the contact point to the ruby hemisphere's center.

For the mobile platform, the steel sphere needs to rotate in two degrees of freedom. A rotation around the vertical rotation axis is not necessary, as it would not change the platforms position. Thus, in the following, only rotations in those two degrees of freedom are considered. If the steel sphere rotates, the contact points move on certain paths (see Fig. 9a).

Since the radii r_{Si} are different for each of those paths, the absolute movement that leads to a specific rotation is

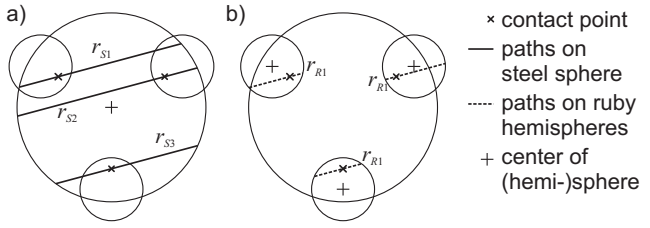

Fig. 9. a) paths on steel sphere, b) and c) paths on ruby hemispheres

different for each contact point. The same applies to the radii r_{Ri} of the contact points on the ruby hemispheres (Fig. 9b). The ratios, however, are identical for each contact point:

$$\frac{r_{R1}}{r_{S1}} = \frac{r_{R2}}{r_{S2}} = \frac{r_{R3}}{r_{S3}} \tag{4}$$

These ratios are also equal to the "gear ratio" between ruby hemispheres and steel spheres. Thus, for a rotation angle α_s of the steel sphere, a ruby hemisphere needs to rotate:

$$\alpha_{Ri} = \frac{r_{Si}}{r_{Ri}} \alpha_S \tag{5}$$

As all $\frac{r_{Si}}{r_{Ri}}$ are equal, all rotation angles α_{Ri} are equal. Thus, to create the same amount of rotation of the steel sphere, all hemispheres need to rotate by the same amount. This is very beneficial as all hemispheres of a steel sphere can be controlled equally by simply connecting their actuator segments in parallel.

Therefore, the sphere can be controlled via three channels exactly as a single ruby hemisphere would be actuated (section 3.1). The only difference is an inversion of direction because the steel sphere always rotates into the opposite direction of a ruby hemisphere.

3.3 Control of the mobile platform

Three steel spheres drive the complete mobile platform. The spheres are arranged in an equilateral triangle in order to simplify both translational and rotational movement. Each steel sphere is controlled via three channels (see section 3.2). This leads to a total of nine channels for the whole mobile platform. Fig. 10 shows examples for translational and rotational movements. Translational movement into an arbitrary direction is achieved by controlling all three steel spheres in parallel. For rotation, the steel spheres have to move on a circle and thus have to move tangentially.

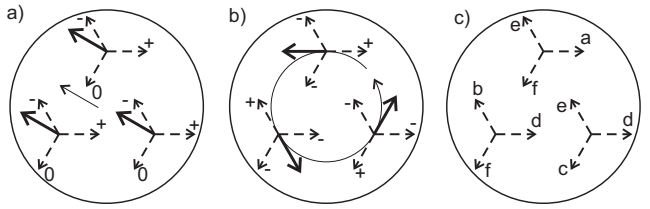

Fig. 10. a) Translational movement, b) rotational movement, c) actuator channels

Using the platform layout in Fig. 10, three pairs of the nine channels can be combined as they are always actuated with the same voltage. This leads to the six channels shown in Fig. 10c).

3.4 Amplification techniques

All segments supporting a ruby hemisphere have been designed to have the same size and shape. This also applies for the cabling delivering the voltages. Thus, all segments have a very similar capacitance, which was measured to be about 100 pF. Actuation channels a, b and c are connected to three segments each, while e, f and g are connected to six segments. Therefore, the channels have a capacitance of 300 pF and 600 pF, respectively.

The stick-slip effect used for actuation is generated by applying saw-tooth shaped signals to the individual segments of the ceramic. There are several key properties of the generated signal. The amplifier of the prototype is able to deliver voltages from −150 V to +150 V. During the slip phase, the amplifier needs to switch from the minimum to the maximum voltage as fast as possible. The maximum slew rate of the amplifier is 400 V/μs and thus the slip can be complete in 750 ns. As the capacitance of each channel is relatively small, even very high signal frequencies are possible. The prototype was tested up to a frequency of 150 kHz.

4. EVALUATION

4.1 Estimated Properties

A key parameter to the evaluation of the mobile platform is the elongation of the individual piezo segments. An FEM simulation has shown that the used ceramic plates extend by 90 nm when a potential of 150 V is applied. Accordingly, the plates contract by 90 nm when with voltage of −150 V. Furthermore, this displacement is directly transfered unscaled to the top of the ruby hemisphere and the top of the steel sphere (see section 3.2). Therefore, the top of the steel sphere and the whole mobile platform can move 90 nm into two opposite directions by applying ±150 V to the segments. During stick-slip actuation, the platform will perform both these movements and a step will have the length of 180 nm. This will correspond to a slip-stick amplitude of 300 Vpp, because each segment is actuated with a signal between -150 V and 150 V.

4.2 Results

To verify the platform's properties, the movement was measured with a laser interferometer. Fig. 11 shows the relation between step length and amplitude at a constant frequency of 1 kHz. The length of ten steps was measured, in order to minimize the effect of measurement errors such as noise and drift as well as acceleration effects. Each measurement was repeated 20 times and the plot shows average, minimum and maximum.

In all measurements, no movement was detected for amplitudes less than 60 Vpp (±30 V on each segment). Between 60 Vpp and 300 Vpp the step lengths increases strictly monotonic and can be approximated by a slow exponential rise.

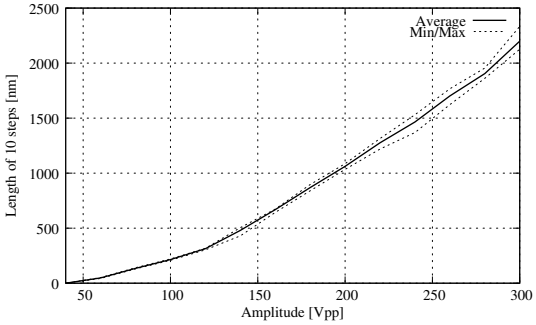

Fig. 11. Measured step length of the platform depending on signal amplitude

Fig. 12 shows the relation between step length and frequency. In order to eliminate the influence of acceleration the measurements show the difference between 40 and 50 steps. Ten measurements were conducted for each frequency and the plots contains average, minimum and maximum. All measurements were conducted at a signal amplitude of 300 Vpp.

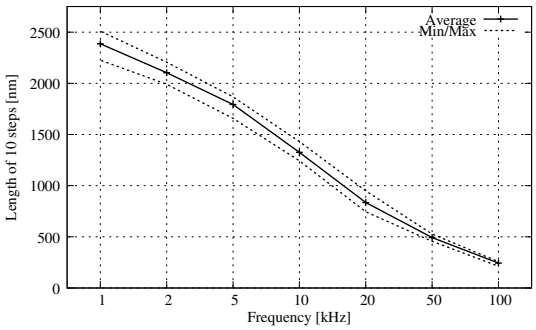

Fig. 12. Measured step length of the platform depending on signal frequency

As can be seen from the plot, the step length decreases with the frequency. This is probably be caused by the hysteretic behavior of the piezo itself as well as dynamic problems of the stick-slip technique.

4.3 Discussion

The measured results match the estimated properties very closely. The small (20%) difference between the theoretic step length of 180 nm at 300 Vpp and the measured length of 220 nm can be explained by two factors. Firstly, the adhesive connecting actuator and ruby hemisphere is very hard to model and is not correctly represented by the assumed point contacts. Secondly, the exact three dimensional movements of the three segments are not entirely known. A carefully planned simulation using the finite element method might help to understand this effect.

5. CONCLUSION

The proposed mobile platform concept has been successfully implemented in a prototype. The created mobile platform is very stiff, has a nm-resolution and a maximum speed of more than 10 mm/s. Furthermore, the stick-slip-effect takes place "inside" the platform which reduces or eliminates special requirements on the working surface. No change in movement properties was noticeable during test on glass, paper or mouse pads. The described approach simplifies the control by reducing the number of channels to six and showing an easy way to achieve both rotational and translational movement

ACKNOWLEDGEMENTS

This work was supported by the European Commission, FP6 Integrated Project NanoHand, IST-5-034274.

REFERENCES

H. Aoyama. Precise miniature robots and desktop flexible production. *Proc. of International Workshop on Microfactories, Japan*, pages 145–156, 1998.

A. Bergander, W. Driesen, A. Lal, T. Varidel, M. Meizoso, H. Bleule, and J.-M. Breguet. Position feedback for microrobots based on scanning probe microscopy. *Proceedings of 2004 IEEE/RSJ International Conference on Intelligent Robots and Systems*, September 2004.

J.-M. Breguet, E. Pernette, and R. Clavel. Stick and slip actuators and parallel architectures dedicated to microrobotics. In *Proc. of SPIE Meeting on Microrobotics: Components and Applications*, volume 2906, pages 13–24, 1996.

A. Burisch, S. Soetebier, J. Wrege, and R. Slatter. Design of a parallel hybrid micro-scara robot for high precision assembly. *Mechatronics & Robotics, Aachen*, 04:1374, 2004.

W. Driesen, T. Varidel, S. Regnier, and J.-M. Breguet. Micro manipulation by adhesion with two collaborating mobile micro robots. *Journal of Micromechanics and Microengineering*, 15:259–267, 2005.

S. Fahlbusch, S. Fatikow, S. Garnica, H. Hülsen, and A. Kortschack. Development of a nanohandling robot cell. *Proc. of the 11th Mediterranean Conference on Control and Automation*, June 2003. T2-008.

S. Fatikow. *Mikrorobotik und Mikrosystemtechnik*, volume 5. University of Oldenburg, Lecture notes, 2004.

S. Fatikow, J. Seyfried, St. Fahlbusch, A. Buerkle, and F. Schmoeckel. A flexible microrobot-based microassembly station. *Journal of Intelligent and Robotic Systems*, (27):135–169, 2000.

H. Hülsen. *Self-Organising Locally Interpolating Maps in Control Engineering.* PhD thesis, University of Oldenburg, Germany, March 2007.

D.-H. Kim, K.-Y. Kim, and K. Kim. A micro manipulation system based on teleoperating techniques. *Proceedings of the 32rd International Symposium on Robotics (ISR 2001)*, July 2001.

A. Kortschack and S. Fatikow. Development of a mobile nanohandling robot. *Journal of Micromechatronics*, pages 249–269, 2004.

S. Martel and I. Hunter. Nanofactories based on a fleet of scientific instruments configured as miniature autonomous robots. *Jornal of Micromechatronics*, 2(3-4):201–214, 2004.

S. Martel, A. Saraswat, and I. Hunter. Fundamentals of piezo-ceramic actuation for micrometer and submicrometer motions for the nanowalker robot. In *SPIE2000*, 2000.

N.N. *Linear Nanopositioners.* PI, Karlsruhe, Germany, 2007.